

Contents lists available at [ScienceDirect](#)

Waste Management

journal homepage: www.elsevier.com/locate/wasman

Model-based prediction of long-term leaching of contaminants from secondary materials in road constructions and noise protection dams

Christof Beyer^{a,b,*}, Wilfried Konrad^b, Hermann Rügner^c, Sebastian Bauer^a, Rudolf Liedl^d, Peter Grathwohl^b

^a Institute of Geosciences, Geohydromodelling, Christian Albrechts University of Kiel, Ludewig-Meyn-Straße 10, 24118 Kiel, Germany

^b Center for Applied Geoscience (ZAG), Eberhard Karls University of Tübingen, Sigwartstraße 10, 72076 Tübingen, Germany

^c Helmholtz-Centre for Environmental Research (UFZ), Permoserstraße 15, 04318 Leipzig, Germany

^d Institute for Groundwater Management, Technische Universität Dresden, 01062 Dresden, Germany

ARTICLE INFO

Article history:

Accepted 19 June 2008

Available online xxx

ABSTRACT

In this study, contaminant leaching from three different secondary materials (demolition waste, municipal solid waste incineration ash, and blast furnace slag) to groundwater is assessed by numerical modeling. Reactive transport simulations for a noise protection dam and a road dam (a typical German autobahn), in which secondary materials are reused as base layers, were performed to predict the breakthrough of a conservative tracer (i.e., a salt) and sorbing contaminants (e.g., PAHs like naphthalene and phenanthrene or heavy metals) at the groundwater table. The dam constructions have a composite architecture with soil covers in inclined layers and distinct contrasts in the unsaturated hydraulic properties of the used materials. Capillary barrier effects result in strong spatial variabilities of flow and transport velocities. Contaminant breakthrough curves at the groundwater table show significant tailing due to slow sorption kinetics and a wide distribution of travel times. While conservative tracer breakthrough depends primarily on subsoil hydraulic properties, equilibrium distribution coefficients and sorption kinetics represent additional controlling factors for contaminant spreading. Hence, the three secondary materials show pronounced differences in the temporal development of leached contaminant concentrations with consequences for breakthrough times and peak concentrations at the groundwater table. Significant concentration reductions due to dispersion occur only if the source concentrations decrease significantly prior to the arrival of the contaminant at the groundwater table. Biodegradation causes significant reduction of breakthrough concentrations only if flow velocities are low.

© 2008 Elsevier Ltd. All rights reserved.

1. Introduction

In many European countries, the reuse of secondary materials like municipal waste incineration ashes or demolition waste in road constructions is promoted by policies and regulations at the national level. In Germany, e.g., the regulation (KrW-/AbfG, 1994) requires – primarily – to prevent waste generation and – secondarily – to recover the material or energy value in the waste generated. Consequently, the reuse of waste has a clear priority over landfilling. For replacement of natural materials in road constructions, recycled granular secondary materials have to meet the same specifications and to provide similar technical properties and performance. Moreover, adverse environmental effects on subsoils and groundwater have to be prevented, i.e., significant leaching of contaminants from recycled wastes is not acceptable, since envi-

ronmental acceptability is a fundamental principle for sustainable recycling. The classification of waste material with regard to soil and groundwater protection is no longer based on total contaminant concentrations measured in the solids. It rather considers the amount of harmful constituents being released under specific scenarios (Schimmoller et al., 2000). Therefore, materials are now characterized by aqueous leaching tests (e.g., Henzler, 2004; Lager et al., 2006; Delay et al., 2007). For example, Stieber et al. (2006) performed detailed unsaturated column experiments with demolition waste on top of different soils under “close-to-field conditions” and observed an efficient attenuation of polycyclic aromatic hydrocarbons (PAHs) in the soil due to microbial degradation, provided the necessary physiological conditions were not impaired by the leachate chemistry (like high pH).

Lysimeter experiments and in-situ field studies are used in order to validate experimental results from the laboratory and to predict the long-term behaviour under natural field conditions. Susset (2007) performed lysimeter studies with layers of demolition waste on top of silty and sandy soil monoliths and observed extended retention of PAHs. Water fluxes in these experiments

* Corresponding author. Address: Institute of Geosciences, Geohydromodelling, Christian Albrechts University of Kiel, Ludewig-Meyn-Straße 10, 24118 Kiel, Germany. Tel.: +49 431 880 3172; fax: +49 431 880 7606.

E-mail address: christof.beyer@gpi.uni-kiel.de (C. Beyer).

were scaled to represent timeframes of several decades under realistic field scenarios. Reduction of salt peak concentrations due to longitudinal dispersion was only observed if the lifespan of the salt source was short in comparison to the overall transport time through the lysimeter. In large-scale field experiments along a road transect in Denmark, Hjelm et al. (2007) observed the development of capillary barriers in the road dam, which caused significant amounts of the seepage water to bypass the secondary material, thus reducing water fluxes through the contaminant source.

These and many other successful field investigations demonstrate the importance of experimental studies on the environmental behaviour of secondary materials. Large-scale in-situ experiments, however, often are very intricate, expensive and time consuming. The application of computer-aided design tools in combination with process-based numerical models can therefore be very beneficial. Process-based numerical models of water flow, reactive contaminant transport and geomechanics have been tremendously improved over the last decade, enabling the simulation of a wide variety of coupled processes and mechanisms relevant in the lifespan of a road construction. Hansson (2005), e.g., developed a mechanistic model of water and heat transport in road structures including freezing and thawing processes and their implications for water movement. Applying numerical simulations of water flow patterns in road dams, Hansson et al. (2006) demonstrated that capillary barriers may result from contrasts in the unsaturated hydraulic properties of the construction materials. Probabilistic simulations of flow and reactive contaminant transport in road embankments were performed by Apul et al. (2005). Recently, Apul et al. (2007) examined the influence of center line and shoulder joints and the effects of damaged pavements on water flow and contaminant leaching in a road cross-section. They described the release of inorganic substances like salts and heavy metals from the secondary materials and the retarded transport in the subsoil by an equilibrium sorption/desorption model.

Apart from salts and heavy metals, secondary materials often contain high amounts of organic contaminants like PAHs. For this class of substances, the equilibrium assumption for the sorption/desorption process may not be appropriate, especially if (a) flow velocities are high (i.e., contact times between seepage water and soil matrix are short), (b) grain diameters are large, and (c) diffusion velocities are small (Grathwohl, 1998). All these conditions are usually satisfied for secondary materials used in road environments. In particular, in coarse grained materials or soils with significant fractions of gravel and rocks, sorption of organic contaminants may be

strongly rate-limited due to intraparticle diffusion (Grathwohl, 1998; Rügner et al., 1997, 1999). Hence, if process based models are to be applied for an evaluation of the environmental impact of organic contaminants from road construction materials, they should be able to take the effects of sorption/desorption kinetics (i.e., non-equilibrium conditions) into account.

In this contribution, we present and apply a numerical modeling approach which is particularly designed for such situations: The finite element model GeoSys (Kolditz and Bauer, 2004; Kolditz et al., 2007) is combined with the Lagrangian stream tube model SMART (Finkel, 1998; Finkel et al., 1998). This allows us (a) to model the complex hydraulics of dam construction geometries consisting of different aggregate materials by the finite element method and (b) to apply the intraparticle diffusion model implemented in SMART for simulating physically realistic release kinetics of secondary material constituents and the intraparticle diffusion limited sorption/desorption kinetics during transport through the vadose zone. The combined model is used to assess and compare the leaching of contaminants from three different secondary materials, which are reused in road and noise protection dams to study the contaminants transport through the vadose zone to the groundwater table. First results for demolition waste (DW) have been presented in Beyer et al. (2007). Here, the study is considerably extended to assess the contaminant leaching behaviour of blast furnace slag (BFS) and municipal solid waste incineration ash (MSWIA) and to set them in relation to the DW. The results of this study support the identification and evaluation of the relevant hydraulic and physiochemical process interactions which are responsible for contaminant attenuation and concentration reduction during transport to groundwater and the observed differences between the various secondary materials.

2. Methods and materials

2.1. Model concept

By combining the numerical models GeoSys and SMART, the simulation problem is split into two sub-problems: simulation of *saturated and unsaturated flow* and simulation of *reactive contaminant transport* (see Fig. 1). The coupling of the flow and reactive transport simulations is achieved by the introduction of probability density functions (pdf) describing the seepage water travel times between different horizontal control planes. The pdfs quantify the influences of hydraulic heterogeneity (i.e., the spatial variability of solute transport velocities) on the flow field (cf. Bold, 2004).

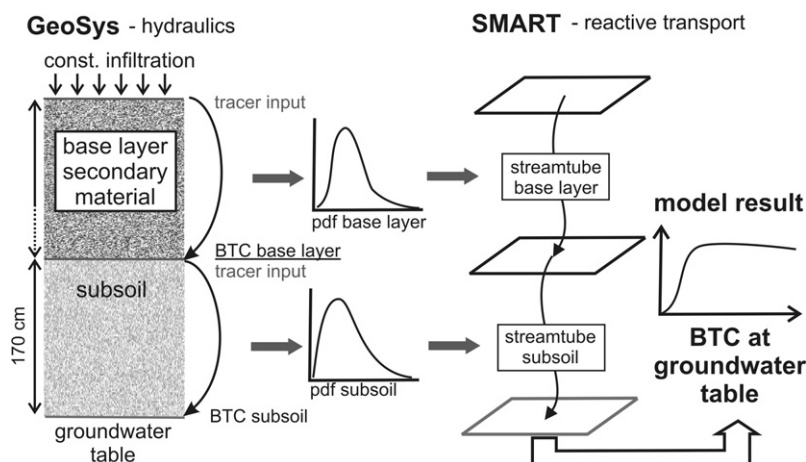


Fig. 1. Model concept: simulation of tracer breakthrough curves for the derivation of travel time distributions (pdf) of separate model layers with GeoSys (left); reactive transport simulations with SMART (right); coupling of both models through the pdf (centre) (modified from Beyer et al. (2007)).

With SMART, layered composite heterogeneous domains are modelled as a sequence of coupled one-dimensional streamtubes. Each streamtube represents one distinct material layer of the model domain (Fig. 1). The solute breakthrough curve obtained at the outlet of a streamtube represents the transient upstream concentration boundary condition for the subsequent streamtube, or – in the case of the lowest streamtube – contaminant input into groundwater.

For each streamtube, a separate pdf has to be generated. To simplify this approach, each streamtube is considered independent from the neighbouring streamtubes (cf. Vanderborght and Vereecken, 2007). The pdfs are derived from synthetic tracer experiments, which are simulated with GeoSys as follows: A conservative tracer with constant concentration $C_0 = 1$ is applied at the upper boundary of each material layer and transported within the flow field. The tracer's breakthrough concentration C at the lower layer boundary is registered over time. The pdf is then obtained as the time derivative dC/dt of the breakthrough concentration plotted over time t .

2.2. Numerical simulation of flow and reactive transport

In GeoSys, the Richards equation is used for the simulation of unsaturated seepage flow (Du et al., 2005). The nonlinear relationships between saturation, pressure head and hydraulic conductivity are described by the van-Genuchten–Mualem model (van Genuchten, 1980; Mualem, 1976). Transport of conservative tracers is simulated using the convection–dispersion-equation. Within the framework of SMART, however, reactive transport is described as a function of travel time along a streamtube (Finkel, 1998). Contaminant attenuation due to sorption or degradation is quantified by the numerical model BESSY (Jaeger and Liedl, 2000) simulating spherical intraparticle diffusion by using Fick's second law:

$$\frac{\partial C_w}{\partial t} = D_a \left[\frac{\partial^2 C_w}{\partial r^2} + \frac{2}{r} \frac{\partial C_w}{\partial r} \right] \quad (1)$$

where r [m] is the radial distance from the grain center, C_w [kg m^{-3}] is the concentration of the aqueous phase within the intraparticle pores, and D_a [$\text{m}^2 \text{s}^{-1}$] is the apparent diffusion coefficient, which is calculated from the aqueous diffusion coefficient D_{aq} by (Grathwohl, 1998):

$$D_a = \frac{D_{aq}\varepsilon}{(\varepsilon + K_d\rho_k)\tau_f} \quad (2)$$

where ε [–] is the intraparticle porosity, τ_f [–] is the tortuosity factor, K_d [$\text{m}^{-3} \text{kg}^{-1}$] is the linear equilibrium distribution or sorption coefficient and ρ_k [kg m^{-3}] is the particle density according to $\rho_k = (1 - \varepsilon)\rho$ with ρ [kg m^{-3}] as the mineral density.

2.3. Model parameterization

In this study, two different construction scenarios are considered: (i) a noise protection dam and (ii) a road dam. In both constructions either municipal solid waste incineration ash (MSWIA), blast furnace slag (BFS) or demolition waste (DW) are considered as secondary materials. Naphthalene and phenanthrene, which are contaminants typically contained in the secondary materials under study, are taken as weakly and strongly sorbing organic contaminants, respectively. We also study the leaching of a conservative tracer. In order to evaluate the influence of subsoil properties on contaminant transport and attenuation, we compare three different subsoils below the constructions. In the following sub-sections, we briefly describe the parameterization of the scenarios. More details can be found in Grathwohl et al. (2006) or Beyer et al. (2007).

2.3.1. Model geometry and secondary materials

The noise protection dam and the road dam are modelled as two-dimensional vertical cross-sections. Due to the symmetry of the constructions, it suffices to perform the simulations only for one-half of the cross-sections.

The geometry of the noise protection dam (Fig. 2) was adopted from a dam studied experimentally by Mesters (1993). The core of the dam consists of BFS, MSWIA or DW. Similarly as Mesters (1993), we assumed that the grain size distribution of the three secondary materials follows the grading curve 0/32 according to FGSV (2004) (Fig. 3). The secondary material is covered by a loam soil.

The road dam model (Fig. 4) was adopted from the cross-section RQ 26 of a typical small scale German autobahn with four lanes (FGSV, 1996). According to FGSV (2005) the side-strip consists of a low permeable loamy sand, while the soil layer covering the embankment is a high permeable sand. The respective soil physical properties are presented in Table 1. The secondary material is used for the unbound base layer and the frost protection layer, which are situated below the road asphalt layer. The subsoil below both the road and the noise protection dam is assumed to have a thickness of 1.7 m.

Experimentally obtained data on unsaturated hydraulic properties of construction materials in road structures are very rare in the literature. Retention and hydraulic conductivity functions of various base materials used in Minnesota (USA) were measured by Bigl and Berg (1996). Their results are, however, not applicable to the

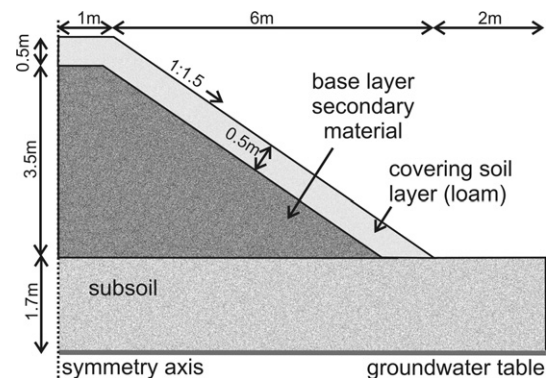


Fig. 2. Noise protection dam with a core consisting of BFS, MSWIA or DW as secondary materials.

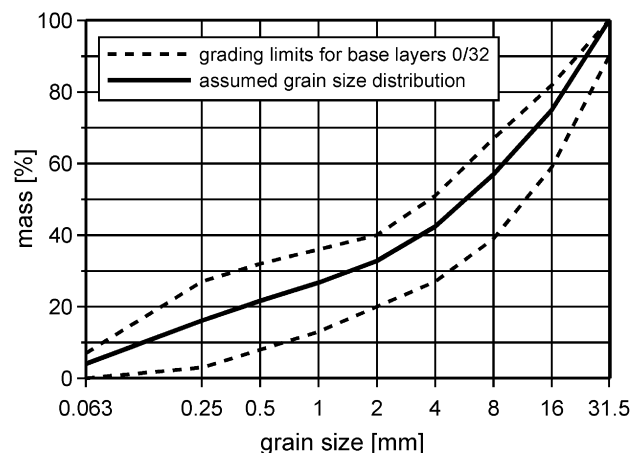


Fig. 3. Grading curve 0/32 (FGSV, 2004) for materials used in unbound base layers in road constructions.

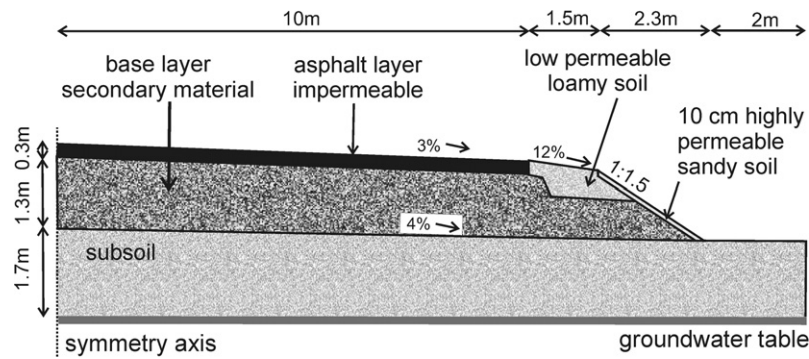


Fig. 4. Road dam with frost protection layer and unbound base layer consisting of BFS, MSWIA or DW as secondary materials.

Table 1
Soil physical properties of the construction materials used in the noise protection dam and in the road dam

	Noise protection dam				Road dam				
	MSWIA	BFS	DW	Embankment ^a	MSWIA	BFS	DW	Side strip ^b	Embankment ^a
θ_s	0.36	0.33	0.31	0.43	0.31	0.28	0.25	0.36	0.37
θ_r	0	0	0	0.08	0.0	0.0	0	0.0	0.04
n	1.29	1.29	1.29	1.56	1.29	1.29	1.29	1.28	1.57
α (m ⁻¹)	186	173	154	3.60	168	155	146	2.64	8.74
l	0.5	0.5	0.5	0.50	0.50	0.50	0.5	0.50	0.50
ρ (g cm ⁻³) ^d	2.83	2.59	2.66	2.65	2.83	2.59	2.66	2.65	2.65
ρ_b (g cm ⁻³)	1.81	1.73	1.84	1.51	1.96	1.87	2	1.69	1.67
ρ_p (g cm ⁻³) ^d	1.9	1.82	1.94	–	1.90	1.82	1.94	–	–
V (–) ^c	0.95	0.95	0.95	–	1.03	1.03	1.03	–	–
K_s (m s ⁻¹)	5.40×10^{-5}	5.40×10^{-5}	5.40×10^{-5}	1.00×10^{-6}	5.40×10^{-5}	5.40×10^{-5}	5.40×10^{-5}	1.00×10^{-6}	2.90×10^{-6}

^a Carsell and Parish (1988).

^b Hennings (2000).

^c FGSV (1997) (noise protection dam), (2004) (road dam).

^d Kellermann (2003).

materials regarded here because they differ with respect to grain size distribution, dry densities and porosities. German road design regulations do not specify any requirements for the retention and hydraulic conductivity functions, apart from the saturated hydraulic conductivity K_s of the base layers, for which FGSV (1998) prescribes a minimum of 5.4×10^{-5} m s⁻¹. Hence, we derived the Van-Genuchten parameters α [m⁻¹], n [–] and l [–], as well as the residual water content θ_r [–] for the secondary materials using an empirical approach of Arya and Paris (1981) and Mishra et al. (1989), which requires information on the grain size distribution, bulk density $\rho_b = (V \cdot \rho_p)$ and porosity $\eta = (1 - \rho_b/\rho)$. V [–] denotes the degree of compaction and ρ_p the proctor density [g cm⁻³] of the aggregate material (cf. Table 1). The saturated water content θ_s [–] was assumed to be identical to the porosity. Although the Arya and Paris method was developed for natural soils, it should – according to Hansson et al. (2006) – also be applicable for relatively coarse grained base layer materials in road constructions. The range of K_s values measured for base layer materials in the laboratory or in field studies is very large (Stoppka, 2002; Kellermann, 2003; Apul et al., 2002). Therefore the minimum value of 5.4×10^{-5} m s⁻¹ as required by FGSV (1998) is used for all scenarios and secondary materials. Fig. 5 shows water content – capillary pressure as well as water content – hydraulic conductivity relations for MSWIA, BFS and DW in the noise protection and road dam scenarios. The hydraulic functions of the different scenarios are similarly shaped. They exhibit a very small capillarity, compared to the soils used for the embankments or the side strip, which ensures a fast drainage of the base layers after heavy rainfall. Differences between the water retention curves for the road

dam and the noise protection dam are due to the different degrees of compaction required in both constructions (cf. Table 1).

Intraparticle porosities ε for the MSWIA, the BFS and the DW, as well as K_d -values of naphthalene and phenanthrene in the three materials were determined experimentally by Henzler (2004) (see Table 2). The aqueous diffusion coefficients D_{aq} were estimated as 7.86×10^{-10} and 9.15×10^{-10} m² s⁻¹, respectively, using the approach of Hayduk and Laudie (1974). The heterogeneous composition of the secondary materials of different grain size fractions was described using the lithocomponent approach of Kleinedam et al. (1999a). The two grain size classes “fine” (32.8% mass fraction) and “coarse” (67.2% mass fraction) were modelled (cf. Rügner et al. 2005), for which sorption kinetics were calculated separately. “Effective” grain radii of $r_{fine} = 0.25$ mm and $r_{coarse} = 8$ mm were assumed (Henzler, 2004).

2.3.2. Subsoil properties

Three different subsoils below the road constructions are considered to evaluate the influence of various natural soil properties (natural barriers) on contaminant breakthrough at the groundwater table: (a) sandy soil with low organic carbon content OC [%] and a large mass fraction of gravel, (b) sandy soil with moderate OC and (c) loess soil with comparably high OC. The properties of the three soils were derived from typical cambisol (a), podzol (b) and chernozem (c) soil profiles described in the German soil survey map 1:1,000,000 (“BÜK1000”; BGR, 2006). As the topsoils are usually removed in road constructions, the properties of the soils compared in this study were derived only from subsoil horizons. To simplify the numerical simulations, the soil profiles between the

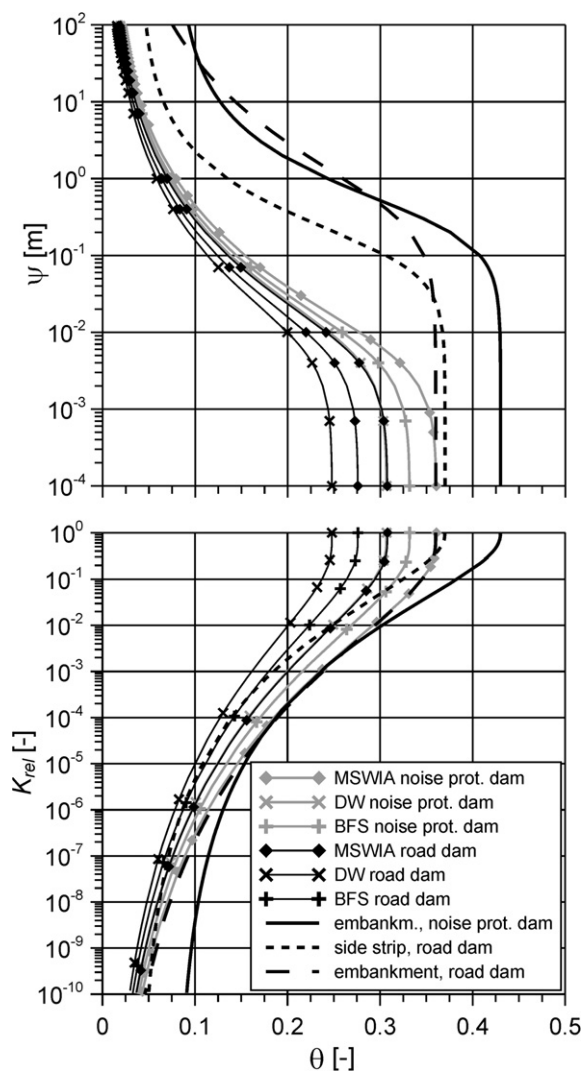


Fig. 5. Water content – capillary pressure (upper diagram) and water content – (relative) hydraulic conductivity relations (lower diagram) for construction materials of the noise protection and the road dam.

Table 2

Intraparticle porosities of DW, MSWIA and BFS and K_d values for naphthalene and phenanthrene in the secondary materials (Henzler, 2004)

	MSWIA	BFS	DW
K_d (L kg ⁻¹) naphthalene	1776	98	166
K_d (L kg ⁻¹) phenanthrene	11598	128	496
Intraparticle porosity ε (-)	0.015	0.015	0.015

base of the road constructions and the groundwater table were assumed as being homogeneous, as a first approximation.

K_s -values and van-Genuchten parameters for the subsoils were estimated from the pedotransfer functions of Wösten et al. (1998) (see Table 3). In the derivation of the pdf from the tracer experiments in GeoSys, longitudinal and transversal dispersivities α_L and α_T of 0.1 m and 0.01 m, respectively, were assumed.

K_d -values for the organic compounds were estimated from the soil mass fraction of organic carbon f_{oc} [-] (=0.01 OC; cf. Table 3) and the OC-normalized distribution coefficient K_{OC} [L kg⁻¹] using the relation $K_d = K_{OC} f_{oc}$. To estimate K_{OC} , the correlation of Seth et al. (1999) was used, which is based on the solubility in water S [mol l⁻¹] (cf. Allen-King et al., 2002):

Table 3
Subsoil properties

Soil type	Subsoil (a) sand, low OC	Subsoil (b) sand, moderate OC	Subsoil (c) loess, high OC
Clay (%)	3.82	10.40	19.69
Silt (%)	14.54	20.48	69.40
Sand (%)	57.41	63.21	8.44
Gravel (%)	24.24	5.91	2.47
OC (%)	0.01	0.21	0.88
ρ_b (g cm ⁻³)	1.71	1.61	1.42
θ_s	0.29	0.36	0.45
θ_s^a	0.01	0.01	0.01
n^a	1.34	1.26	1.15
α^a (m ⁻¹)	5.93	5.98	1.76
β^a	1.77	-0.30	-1.91
K_s^a (m s ⁻¹)	1.52×10^{-6}	3.37×10^{-6}	3.83×10^{-6}
K_d^b (L kg ⁻¹) naph.	5.8×10^{-2}	1.20	5.10
K_d^b (L kg ⁻¹) phen.	0.98	20.00	87.00

^a Derived according to Wösten et al. (1998); K_s corrected for gravel content according to Brakensiek and Rawls (1994).

^b For the fine fraction.

$$\log K_{OC} = -0.88 \log S + 0.07 \quad (3)$$

S is 3.46×10^{-5} mol l⁻¹ for phenanthrene and 8.74×10^{-4} mol l⁻¹ for naphthalene. For the gravel fractions, $\log K_{OC}$ values of 4.0 (naphthalene) and 5.2 (phenanthrene) were assumed (Rügner et al., 2005), as the OC in coarse limestone or sandstone fragments usually consists of aged organic material with higher sorption capacity (Kleineidam et al., 1999b); f_{oc} was assumed as 0.0005 (Kleineidam et al., 1999b).

The sorption kinetics of the fine soil is mainly governed by the particular organic material. Here, effective parameters for the grain radius $r = 11.7 \mu\text{m}$, $\varepsilon = 0.00175$, $\rho = 2.65 \text{ g cm}^{-3}$ and the tortuosity $\tau_f = 1/\varepsilon$ were assumed (Grathwohl, 1992; Rügner et al., 1999). For the gravel fraction (>2 mm), the values $r = 1 \text{ cm}$ and $\varepsilon = 0.01$ were assigned (Rügner et al., 1999; Kleineidam et al., 1999a).

In the presence of dissolved organic matter (DOM) PAHs are known to show increased leaching rates due to sorption and co-transport on the DOM (e.g., Kim and Osako, 2003). Alkaline conditions, which may develop in the leachate, e.g., in the presence of concrete constituents in DW, favour the dissolution of soluble organic carbon and hence could result in reduced sorption of the PAHs to the soil matrix and accelerated breakthrough at the groundwater surface. These processes, however, could not be included in the prognosis simulations, as this would require a coupling of the transport model with detailed geochemical models of the soils buffering behaviour and DOM concentrations as functions of soil solution pH and, in addition, the data basis necessary for a parameterisation of these processes is lacking.

The transport simulations for naphthalene and phenanthrene were performed once with and once without accounting for the effects of biodegradation. Biodegradation was assumed to be limited to the dissolved fraction only and was modelled as a first order degradation kinetics. Due to the complexity of the interactions between contaminant specific properties, climatic and geochemical boundary conditions (e.g., temporally increasing soil pH from concrete constituents in DW) (Grathwohl et al., 2003; Höhener et al., 2006; Stieber et al., 2006), reliable estimation of representative long-term degradation rate constants remains difficult (Henzler et al., 2006). Therefore, a constant and relatively low value of $1.15 \times 10^{-7} \text{ s}^{-1}$ (half life = 70 d) was assumed as a conservative estimate.

2.3.3. Initial and boundary conditions

For the long-term assessment of contaminant leaching, it is reasonable to assume simplified flow conditions (Grathwohl and

Susset, 2001; Henzler et al., 2006). Hence, stationary flow fields are assumed. For the upper boundary condition, mean annual infiltration rates I [mm a^{-1}] for Germany were estimated using the method of Glugla et al. (2003). For the noise protection dam we obtained $I = 313 \text{ mm a}^{-1}$. For the road dam, the surface runoff on the asphalt layer is infiltrated along the side-strip and the embankment. Since the road dam cross-section was modelled according to a recent regulation (FGSV, 2005) and since no experimental infiltration data are available at present, it was assumed that infiltration is homogeneously distributed along the side-strip and embankment with $I = 2318 \text{ mm a}^{-1}$. For the base of the embankment, we assumed $I = 313 \text{ mm a}^{-1}$, as for the noise protection dam. For the lower model boundary (i.e., the groundwater table), a constant pressure boundary condition $\psi = 0 \text{ m}$ was chosen.

As the distribution of contaminants between the dissolved (bulk pore and intraparticle pore water) and the solid phase (sorbed fraction) is described by a linear sorption isotherm and first order kinetics are assumed for contaminant degradation, the mathematical model describing the contaminant concentrations in the seepage water is linear under stationary flow conditions. Hence, there exists a proportionality between the dissolved contaminant concentration $C(x, t)$ and the initially sorbed concentration C_0 in the contaminant source (i.e., the secondary material). Therefore relative concentrations of $C_0 = 1.0$ were used as initial conditions for naphthalene, phenanthrene and for the conservative tracer in the secondary material. Elsewhere, $C_0 = 0.0$ was used. For the initial pressure distribution, the steady state pressure distribution was used.

3. Results and discussion

3.1. Hydraulics of the noise protection and road dams

Although the hydraulics of the noise protection and road dam is not the main focus of this paper, a brief characterisation is necessary here in order to facilitate the interpretation of the results of the transport simulations. For a more detailed discussion, we refer to Beyer et al. (2007).

The composite architecture of both constructions with inclined boundaries of material layers and the strongly contrasting hydraulic soil properties (see Figs. 2, 4 and 5) result in a complex hydraulic behaviour under unsaturated conditions. On the horizontal top of the noise protection dam, seepage from the loam into the secondary materials is unhindered. Along the inclined embankment, however, the combined layers of fine grained loam and coarse grained secondary materials act as a capillary barrier, which causes

the seepage water to partially bypass the core of the dam and thus reduces the infiltration into the secondary materials (Fig. 6a). The spatial variability of seepage fluxes results in a complex pattern of flow velocities in the secondary materials and the subsoil below the dam. Below the top of the dam, moderate flow velocities prevail. In the immediate proximity, flow velocities are lowest, as the infiltration is hindered by the capillary barrier in the upper part of the embankment. Flow velocities are highest at the outer base of the embankment, since infiltration is focussed in this area.

As the surface runoff on the asphalt layer of the road dam is infiltrated along the side-strip and the embankment, water fluxes are in general much higher than for the noise protection dam. Nonetheless, capillary barriers are also observed in the embankment of the road dam. Along the side-strip, however, seepage infiltration from the loamy sand into the secondary materials is more or less uniformly distributed, as here the material boundary is not much inclined. Again seepage fluxes in the secondary materials show a distinct pattern of spatial variability with high flow velocities below the side strip, low velocities below the embankment and very high flow velocities near its outer base, where infiltration is focussed (Fig. 6b).

As the water content – capillary pressure and the water content – hydraulic conductivity relations for MSWIA, BFS and DW are very similar (Fig. 5), differences in the hydraulic behaviour with regard to the secondary material used for the base layers in the dam constructions in general are very small (cf. Grathwohl et al., 2006).

3.2. Conservative tracer transport

Fig. 7 presents breakthrough curves of the conservative tracer at the groundwater table calculated with SMART with MSWIA as secondary material on top of the three different subsoils (for the noise protection dam see Fig 7a, for the road dam see Fig 7b). According to the streamtube concept of SMART, the model domains of the noise protection dam and the road dam are represented as one-dimensional streamtubes (cf. Section 2.1). Hence, the breakthrough curves obtained with SMART are not representative for discrete locations at the lower model boundary but represent concentrations integrated along the lower model boundaries of the contaminant transport path (see dashed grey lines and double arrows in Fig. 6). For the noise protection dam, breakthrough of tracer peak concentrations is between 2.2 a (low and moderate OC sand) and 3.6 a (loess). The later breakthrough of the tracer peak for the loess in comparison to both sands reflects the contrasts in unsaturated hydraulic properties between the subsoils, i.e., the slower pore water velocities in the loess. Dispersion reduces tracer concentra-

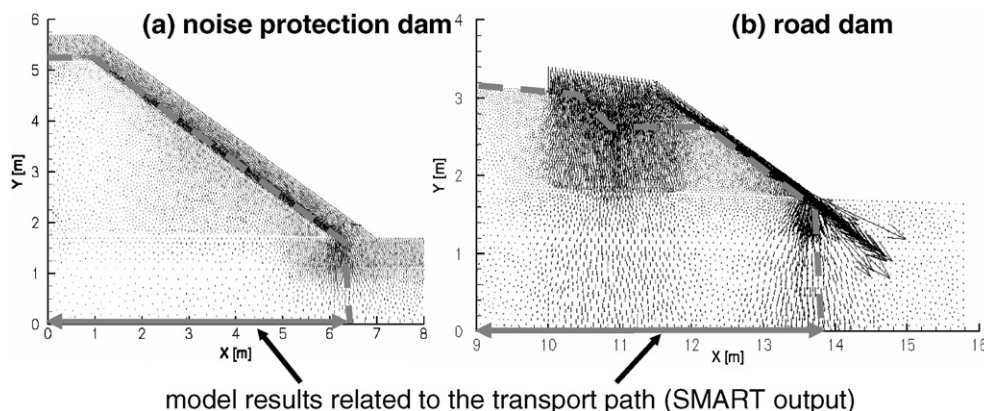


Fig. 6. Flow velocity in the noise protection dam (a) and the road dam (b). The dashed grey lines indicate the envelopes of the “transport path” for which the SMART simulation yields model output (concentrations integrated along the double arrows at the lower model boundary) (modified from Beyer et al. (2007)).

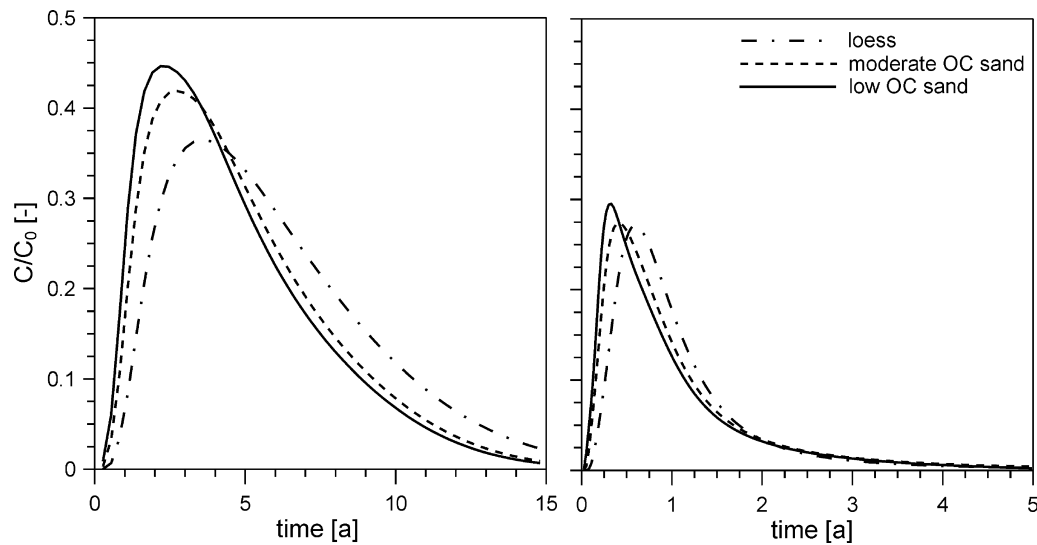


Fig. 7. Conservative tracer breakthrough curves for the noise protection dam (left diagram) and the road dam (right diagram) with municipal solid waste incineration ash as base layer and three different subsoils.

tions to C/C_0 between 0.42 (low OC sand) and 0.36 (loess). Due to the spatial variability of flow velocities in the noise protection dam, the breakthrough curves show substantial tailing. This is because the leaching of the tracer from zones with reduced water fluxes (e.g., below the embankment) takes considerable time. After 10 a, C/C_0 is still as high as 0.11 for the loess.

Although flow velocities in the road dam are generally much higher than in the noise protection dam – peak breakthrough times are between 0.3 a (low and moderate OC sand) and 0.6 a (loess) – a significant tailing of the breakthrough curves is observed also here. Due to increased dispersion from higher flow velocities, peak breakthrough concentrations C/C_0 vary between 0.27 and 0.30 and are somewhat lower than for the noise protection dam. If the peak breakthrough times and concentrations of the tracer leaching simulations for MSWIA as the base layer material are compared to those obtained for BFS or DW (Tables 4 and 5; Beyer et al., 2007), very similar results are found. As the leaching of the tracer is not kinetically limited and transport is unretarded, breakthrough times and concentrations are solely determined by the hydraulic characteristics of the constructions and the spatial variabilities of the water fluxes, which do not differ much between the three secondary materials compared in this study.

The tracer transport simulations with peak breakthrough concentrations C/C_0 as high as 0.44 suggest that immissions of readily soluble and non- (or very weakly) sorbing salts like chloride or lithium from secondary materials used in road constructions to the groundwater might reach concentration levels significantly above legal limits for time periods of several years. Non-tolerable concentrations in groundwater may last even longer for salts like sulfate, which are known to show stronger retardation in soils. These results are in accordance with outcomes of experimental lysimeter studies by Susset (2007).

3.3. Reactive transport of naphthalene and phenanthrene

The reactive transport simulations for naphthalene and phenanthrene without biodegradation were run for a period of 300 a. Fig. 8(a–c) present the resulting breakthrough curves for naphthalene at the groundwater table. Each diagram depicts the results for the three secondary materials MSWIA, BFS and DW in the noise protection dam (grey curves) and in the road dam (black curves). Fig. 8a is related to the low OC sand, (b) and (c) to the moderate OC sand and the high OC loess soil, respectively. Fig. 8(d–e) show the corresponding breakthrough curves for phenanthrene.

Table 4

Breakthrough times (BTT) and peak concentrations at the groundwater table for the tracer, naphthalene and phenanthrene below the noise protection dam (BTT and peak concentrations for the simulations with biodegradation are given in parentheses)

Tracer	Naphthalene			Phenanthrene					
	BTT _{C/C0 = 0.1}	BTT _{peak}	C/C ₀ (peak)	BTT _{C/C0 = 0.1}	BTT _{peak}	C/C ₀ (peak)			
<i>Subsoil (a) low OC sand</i>									
BFS	0.7	2.2	0.44	2.2 (– ^a)	154.0 (16.7)	0.89 (0.03)	17.8 (– ^a)	>300 ^b (51.3)	>0.56 ^b (0.03)
MSWIA	0.7	2.2	0.45	2.2 (– ^a)	>300 ^b (78.6)	>0.98 ^b (0.04)	17.8 (– ^a)	>300 ^b (>300 ^b)	>0.61 ^b (>0.05 ^b)
DW	0.7	2.2	0.43	2.2 (– ^a)	188.2 (26.3)	0.93 (0.03)	17.8 (– ^a)	>300 ^b (118.6)	>0.63 ^b (0.04)
<i>Subsoil (b) moderate OC sand</i>									
BFS	0.8	2.7	0.41	8.0 (– ^a)	110.1 (17.0)	0.92 (0.03)	125.8 (– ^a)	>300 ^b (156.7)	>0.33 ^b (0.02)
MSWIA	0.8	2.7	0.42	8.2 (– ^a)	215.6 (32.3)	0.99 (0.03)	123.8 (– ^a)	>300 ^b (>300 ^b)	>0.35 ^b (>0.03 ^b)
DW	0.8	2.5	0.41	7.9 (– ^a)	129.3 (20.3)	0.95 (0.03)	123.8 (– ^a)	>300 ^b (225.6)	>0.39 ^b (0.03)
<i>Subsoil (c) loess</i>									
BFS	1.2	3.6	0.36	32.6 (– ^a)	>300 ^b (41.9)	>0.87 ^b (0.01)	>300 ^b (– ^a)	>300 ^b (>300 ^b)	>0.02 ^b (>0.01 ^b)
MSWIA	1.2	3.6	0.37	32.3 (– ^a)	>300 ^b (64.7)	>0.95 ^b (0.01)	>300 ^b (– ^a)	>300 ^b (>300 ^b)	>0.02 ^b (>0.01 ^b)
DW	1.2	3.3	0.35	32.3 (– ^a)	300.0 (48.8)	0.93 (0.01)	>300 ^b (– ^a)	>300 ^b (>300 ^b)	>0.03 ^b (>0.01 ^b)

^a Maximum observed concentration is below the $C/C_0 = 0.1$ level.

^b Concentration maximum is not reached within 300 a of simulation time.

Table 5
Breakthrough times (BTT) and peak concentrations at the groundwater table for the tracer, naphthalene and phenanthrene below the road dam (BTT and peak concentrations for the simulations with biodegradation are given in parentheses)

	Tracer			Naphthalene			Phenanthrene		
	BTT _{C/C₀ = 0.1}	BTT _{peak}	C/C ₀ (peak)	BTT _{C/C₀ = 0.1}	BTT _{peak}	C/C ₀ (peak)	BTT _{C/C₀ = 0.1}	BTT _{peak}	C/C ₀ (peak)
<i>Subsoil (a) low OC sand</i>									
BFS	0.1	0.3	0.28	0.3 (0.3)	14.3 (5.3)	0.80 (0.28)	1.92 (2.6)	40.7(17.7)	0.58 (0.22)
MSWIA	0.1	0.3	0.30	0.3 (0.4)	120 (41.6)	0.98 (0.31)	2.0 (2.7)	>300 ^b (274.0)	>0.91 ^b (0.31)
DW	0.1	0.3	0.26	0.3 (0.3)	22.6 (8.9)	0.85 (0.29)	1.9 (2.5)	102.9 (46.7)	0.74 (0.27)
<i>Subsoil (b) moderate OC sand</i>									
BFS	0.2	0.4	0.25	1.6 (2.0)	17.8 (8.5)	0.85 (0.25)	26.0 (35.2)	132.9 (74.2)	0.51 (0.16)
MSWIA	0.2	0.4	0.27	1.6 (2.0)	95.5 (19.2)	0.98 (0.28)	25.4 (31.5)	>300 ^b (224.5)	>0.92 ^b (0.28)
DW	0.2	0.4	0.24	1.6 (2.0)	23.1 (10.1)	0.90 (0.27)	25.5 (32.0)	203.8 (109.6)	0.76 (0.23)
<i>Subsoil (c) loess</i>									
BFS	0.3	0.6	0.27	7.3 (10.7)	41.5 (23.0)	0.79 (0.16)	129.7 (– ^a)	>300 (238.7)	>0.34 ^b (0.07)
MSWIA	0.3	0.6	0.28	7.2 (10.3)	120.2 (38.2)	0.98 (0.20)	119.5 (170.2)	>300 ^b (>300 ^b)	>0.47 ^b (>0.17 ^b)
DW	0.3	0.6	0.27	7.2 (10.4)	52.9 (26.9)	0.88 (0.18)	121.0 (188.4)	>300 ^b (>300 ^b)	>0.49 ^b (>0.13 ^b)

^a Maximum observed concentration is below the C/C₀ = 0.1 level.

^b Concentration maximum is not reached within 300 a of simulation time.

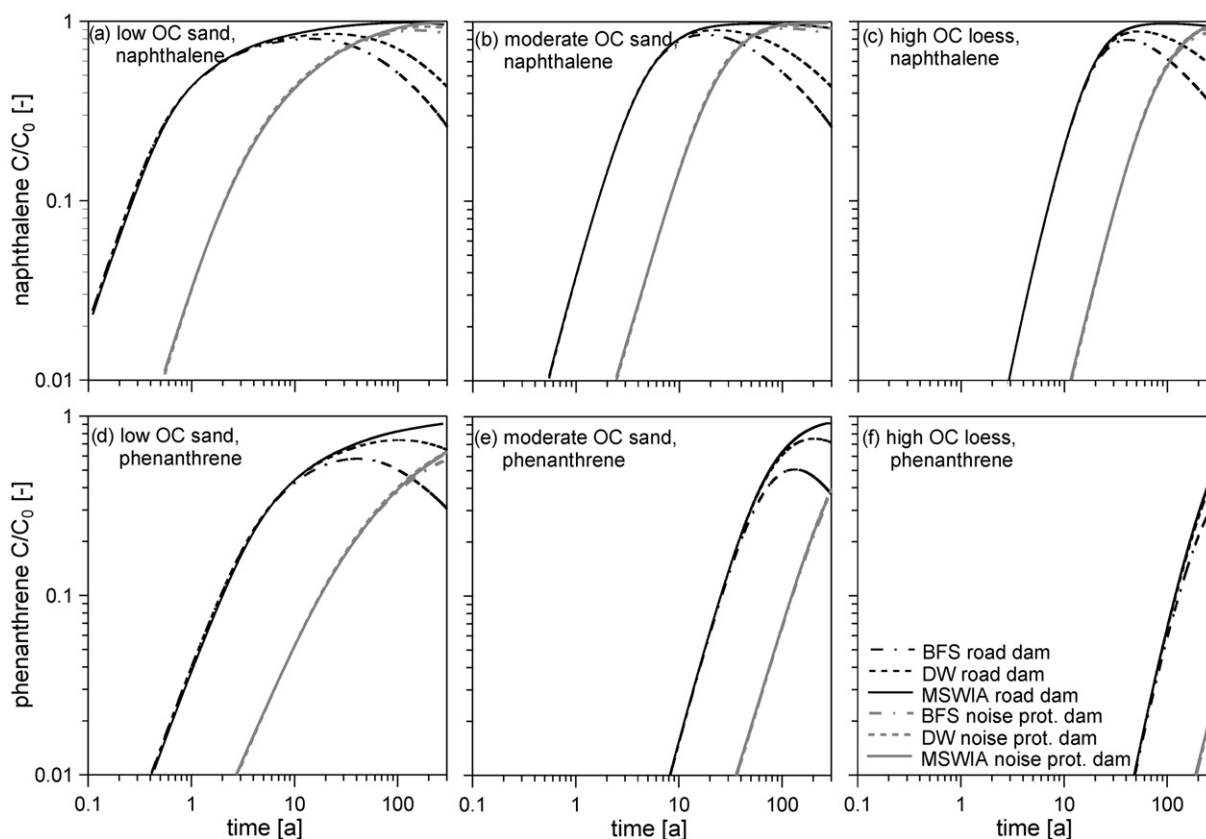


Fig. 8. Breakthrough curves of naphthalene (a, b, c) and phenanthrene (d, e, f) for the noise protection dam (grey curves) and the road dam (black curves) with three different subsoils. Please note that logarithmic axes are used.

As already observed in the transport simulations of the conservative tracer, the very high infiltration rates in the road dam side-strip and the embankment cause a much faster solute breakthrough as compared to the noise protection dam. While naphthalene breakthrough concentrations for the noise protection dam on top of the low OC sand (Fig. 8a) exceed a relative concentration $C/C_0 = 0.1$ after approximately 2.2 a with all secondary materials, for the road dam only 0.3 a are required to reach this concentration level. Naphthalene peak breakthrough for the road dam with BFS as base layer material is reached after 14.3 a with $C/C_0 = 0.80$. After the peak breakthrough, naphthalene concentra-

tions at the groundwater table slowly decrease and reach levels of $C/C_0 = 0.26$ at the end of the simulation. In contrast, the peak breakthrough time with MSWIA as base layer material is approximately 120 a and $C/C_0 = 0.98$ (see Table 5). After 300 a, C/C_0 is still as high as 0.96. The behaviour of the DW is in between these two materials, with a peak concentration of $C/C_0 = 0.85$ being reached after 22.6 a and $C/C_0 = 0.43$ at the end of the simulation. Fig. 9 presents naphthalene concentrations directly below the different secondary materials in the road dam and in the noise protection dam. For the road dam the much faster decrease of naphthalene concentrations leached from BFS (and DW) with $C/C_0 = 0.25$ after 300 a

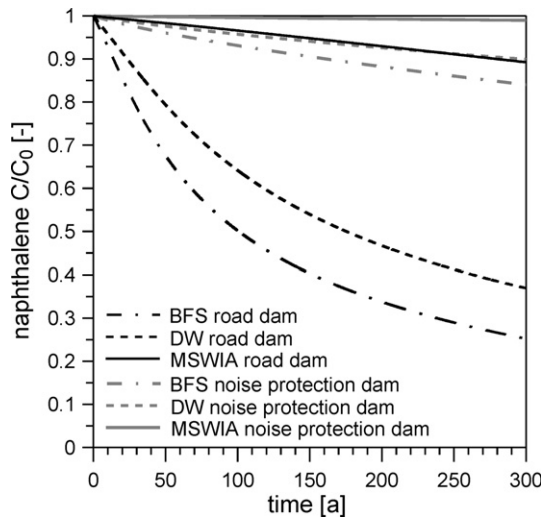


Fig. 9. Temporal development of naphthalene concentrations (without biodegradation) leaching from the various secondary materials studied for the noise protection dam and the road dam.

(DW: $C/C_0 = 0.37$) in comparison to MSWIA ($C/C_0 = 0.89$) is obvious. The significantly longer time period required for the depletion of naphthalene in the MSWIA is a consequence of its high K_d value, which is approximately one order of magnitude larger than for the BFS and the DW (see Table 2).

The comparably fast decrease of leachate concentrations from the BFS and the DW is also the reason for the lower peak breakthrough concentrations at the groundwater table observed for

these materials. If source leachate concentrations decrease significantly before the contaminant peak reaches the groundwater table, the peak breakthrough concentration may be reduced by longitudinal dispersion. For the MSWIA in the road dam, source leachate concentrations are on a high level throughout the whole simulated time period. As a consequence, this material shows the highest breakthrough concentrations C/C_0 .

With respect to the noise protection dam, the temporal development of source concentrations shows a less distinct influence on the height of the breakthrough peaks. The reason for this behaviour is that water fluxes through the secondary material are much lower, hence, it takes a longer time to deplete the initial contaminant load. Accordingly, after 300 a concentrations directly below the naphthalene source are still as high as $C/C_0 = 0.84$ (BFS), 0.99 (MSWIA) and 0.90 (DW) and naphthalene breakthrough curves at the groundwater table appear very similar for the three secondary materials (Fig. 8a). Concentration peaks are reached for the BFS after 154 a with $C/C_0 = 0.89$ and for the DW after 188 a with $C/C_0 = 0.92$. For MSWIA, a value of $C/C_0 = 0.98$ is reached at the end of the simulation, and concentrations still increase slightly.

Qualitatively similar results are obtained for the moderate OC sand and the high OC loess as subsoils. Comparing the respective breakthrough curves (Fig. 8a–c), however, the effect of subsoil OC dependent sorption is obvious: While breakthrough of low to moderate naphthalene concentrations is rather fast for the low OC sand (Fig. 8a), retardation in the moderate OC sand (Fig. 8b) and the high OC loess (Fig. 8c) is stronger. With the moderate OC sand, the $C/C_0 = 0.1$ concentration level is exceeded after approximately 7.9–8.2 a (noise protection dam) and 1.6 a (road dam), respectively. For the high OC loess, the corresponding breakthrough times are between 32.3–32.6 a and 7.2–7.3 a. Also the peak breakthrough times are later for the moderate OC sand and the loess. Differences

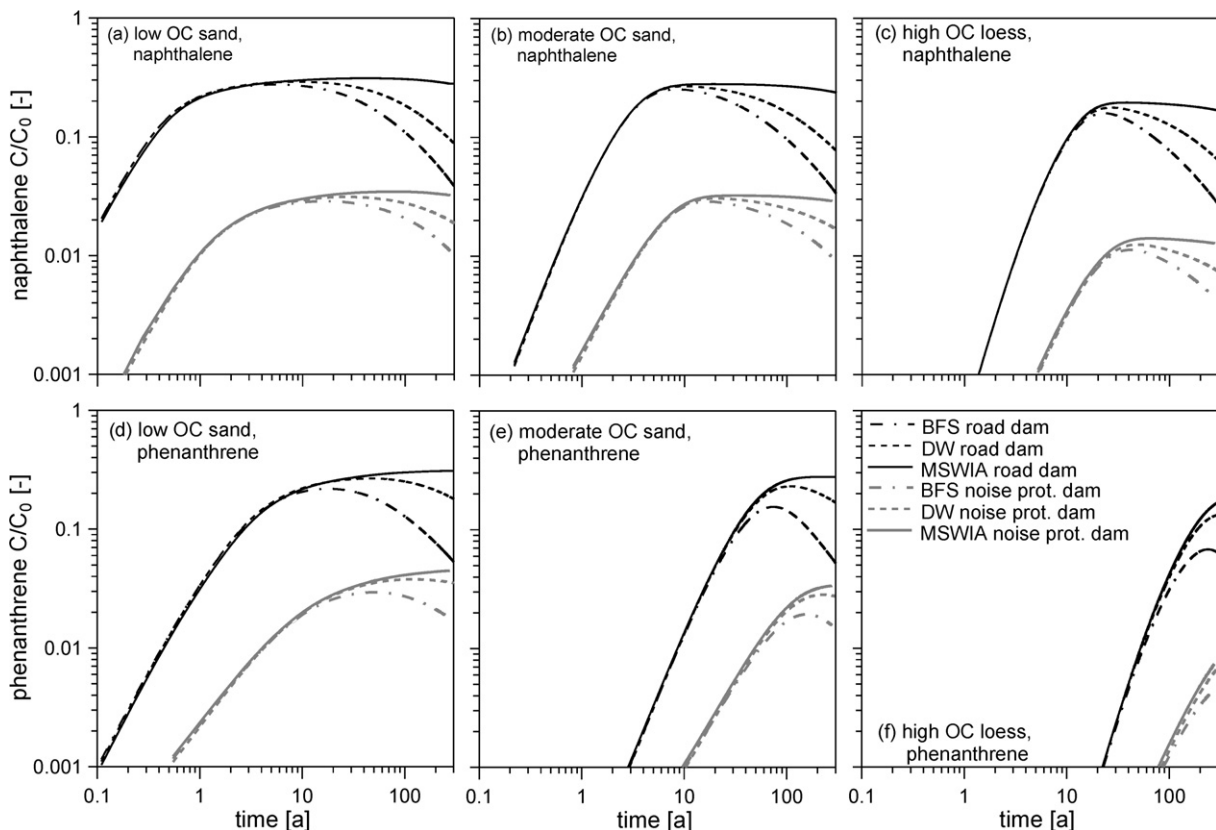


Fig. 10. Breakthrough curves of naphthalene (a, b, c) and phenanthrene (d, e, f) with biodegradation for the noise protection dam (grey curves) and the road dam (black curves) in three different subsoils. Please note that logarithmic axes are used.

between the two sands, however, are not as pronounced as for the $C/C_0 = 0.1$ concentration level (see Tables 4 and 5). The breakthrough curves for the low OC sand show a slight tailing for concentrations $C/C_0 > 0.5$ in comparison to the other two subsoils. This is a consequence of the larger gravel fraction of the low OC sand, for which sorption is limited by intraparticle diffusion kinetics.

For phenanthrene, the low OC sand also shows distinct retardation (Fig. 8d). Breakthrough times for the $C/C_0 = 0.1$ concentration level are approximately 17.8 a for the noise protection dam and from 1.9 to 2.0 a for the road dam. Again, the slight tailing of the breakthrough curves for $C/C_0 > 0.5$ shows the influence of the intraparticle diffusion limited sorption kinetics in the gravel fraction of the soil. Due to the stronger retardation of phenanthrene in the subsoil, breakthrough of the concentration peaks within the simulated time of 300 a is only observed for the road dam with BFS or DW as base layer material and with low or moderate OC sands as subsoils. For the other scenarios, especially for the noise protection dam, all simulations show still increasing phenanthrene breakthrough concentrations after 300 a of simulation time. With the loess subsoil, C/C_0 is still less than 0.03 at the end of the simulation for all secondary materials.

Despite the retardation of organic contaminants in soils containing at least small amounts of OC, the complete mobile contaminant mass of the secondary materials is leached to the groundwater in the long run if biodegradation is not accounted for. With biodegradation in the numerical simulations (Fig. 10a–f), the mass reduction for a given degradation rate constant is dependent on the residence time of the dissolved contaminant in the mobile water phase of the soil. Consequently, differences in breakthrough concentrations between the noise protection dam and the road dam are very distinct: Due to the lower infiltration rates and slower flow velocities in the noise protection dam, the average residence time of dissolved contaminants in the unsaturated zone is significantly longer than for the road dam scenario. This results in a higher reduction of the concentrations. In relation to the simulations without biodegradation, breakthrough concentrations for the noise protection dam are reduced by factors between 29 and 78, while for the road dam much smaller reduction factors between 2.5 and 5 are found. For the same reason, an increased mass reduction is observed for the loess soil in comparison to the two sand soils (Tables 4 and 5). Pore water velocities are lower in the loess than in the sand soils, and hence, residence time of the dissolved contaminants in the vadose zone are longer for a given soil profile depth. Retardation from sorption to the soil matrix has no influence on the degraded mass fraction as biodegradation was assumed to be limited to the dissolved fraction only.

Comparing the results for the three secondary materials, for MSWIA in general the highest peak concentrations are found. Moreover, breakthrough concentrations persist on the peak level for very long time spans, i.e. at least until the end of the simulated period of 300 a. The lowest peak breakthrough concentrations are found for BFS, showing a clear decrease within several decades.

Biodegradation has also a strong influence on the contaminant concentrations leaching from the secondary materials. Fig. 11 presents naphthalene concentrations (including biodegradation) directly below the various secondary materials in the road dam and in the noise protection dam. Naphthalene concentrations are significantly lower than those for the equivalent simulations without biodegradation (Fig. 9). Especially for the road dam, biodegradation within the contaminant source has a noticeable effect on breakthrough concentrations at the groundwater table. Here, the breakthrough of both the naphthalene and phenanthrene concentration peaks, is observed within the simulated time of 300 a for BFS and DW as secondary materials on top of the sand soils, while

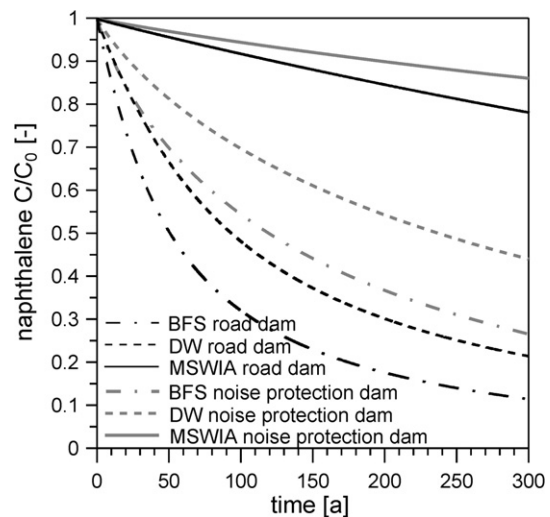


Fig. 11. Temporal development of naphthalene concentrations (with biodegradation) leaching from the different secondary materials studied for the noise protection dam and the road dam.

for the no-biodegradation simulations, breakthrough concentrations were still increasing after 300 a.

4. Conclusions

The numerical simulations performed in this study for the road dam and the noise protection dam show a complex interaction of unsaturated flow and reactive transport processes. We observed a strong influence of the spatial variability of water fluxes on overall contaminant transport. Regions with high flow velocities result in early arrival times of contaminants at the groundwater table, while regions with low flow velocities cause a long tailing of the breakthrough curves. Transport predictions neglecting these effects might underestimate short-term as well as long-term contaminant leaching to groundwater and might thus not be conservative.

For the three secondary materials, municipal solid waste incineration ash, blast furnace slag and demolition waste, that have been compared in this study, strong differences were found in the temporal contaminant leaching behaviour. These can be mainly attributed to their different sorption strength with regard to the contaminants. The temporal development of the leaching of the source material has consequences for the contaminant breakthrough in the subsoil: For example, dispersion reduces contaminant concentrations significantly only if source concentrations decrease significantly before contaminant breakthrough at the groundwater table occurs. Dispersion of easily soluble salts may represent an effective mechanism of concentration reduction because they are leached from the secondary materials within short time periods as compared to their transport time in the unsaturated subsoil, if groundwater levels are sufficiently distant from the contaminant source. On the other hand, if source concentrations of persistent substances stay on high levels for long time periods, an almost unreduced concentration breakthrough can be expected.

For strongly sorbing contaminants under “natural” groundwater recharge conditions, a retardation of peak breakthrough times up to several decades or even centuries can be expected even for subsoils with low organic carbon content. Moreover, if residence times of the seepage water in the unsaturated zone are large enough, a significant reduction of breakthrough concentrations of organic contaminants is possible through biodegradation, even if

degradation rate constants are relatively low. For road environments with high seepage velocities due to focussed surface runoff infiltration, however, biodegradation may be rather limited.

The strong contrast in unsaturated hydraulic properties between the secondary materials and the covering soils used along the embankment and the road side strip generate capillary barrier effects. With appropriate construction geometries and soil materials, these could be enhanced to achieve a further reduction of infiltration into the secondary materials. In this sense, the modelling approach presented in this study allows an optimisation of the design of road constructions with regard to minimal environmental impact and maximum possible reuse of industrial by-products. The major requirement for such a task, however, is substantial knowledge about the exact hydraulic behaviour of these materials under unsaturated conditions. Therefore, future research on the appropriateness of secondary materials or industrial by-products for reuse in road environments should include an effort to provide reliable means for their hydraulic characterisation to improve the effectiveness of capillary barriers.

Acknowledgements

This work was funded by the German Ministry of Education and Research (BMBF) under Grant 02WP0517 as part of the Sickerwasserprognose priority program. We gratefully acknowledge C.H. Park, J. Utermann, W. Duijnvisveld, B. Susset, W. Leuchs, R. Henzler and B. Kocher for their help and constructive discussions. We would also like to thank C.S. Poon and the two anonymous reviewers for their helpful suggestions and comments on the manuscript.

References

- Allen-King, R.M., Grathwohl, P., Ball, W.P., 2002. New modelling paradigms for the sorption of hydrophobic organic chemicals to heterogeneous carbonaceous matter in soils, sediments and rocks. *Advances in Water Resources* 25, 985–1016.
- Apul, D.S., Gardner, K.H., Eighmy, T.T., 2007. Modeling hydrology and reactive transport in roads: The effect of cracks, the edge, and contaminant properties. *Waste Management* 27 (10), 1465–1475.
- Apul, D.S., Gardner, K.H., Eighmy, T.T., Benoit, J., Brannaka, L., 2002. A review of water movement in the highway environment: Implications for recycled materials use. Report to Federal Highways Administration, Recycled Materials Resource Center, University of New Hampshire, Durham NH, USA.
- Apul, D.S., Gardner, K.H., Eighmy, T.T., Linder, E., Frizzell, T., Roberson, R., 2005. Probabilistic modeling of one dimensional water movement and leaching from highway embankments containing secondary materials. *Environmental Engineering Science* 22 (2), 249–262.
- Arya, L.M., Paris, J.F., 1981. A physicoempirical model to predict soil moisture characteristics from particle-size distribution and bulk density data. *Soil Science Society of America Journal* 45, 1023–1030.
- Beyer, C., Konrad, W., Rügner, H., Bauer, S., Park, C.H., Liedl, R., Grathwohl, P., 2007. Modellbasierte Sickerwasserprognose für die Verwertung von Recycling-Baustoff in technischen Bauwerken (Model-based prognosis of contaminant leaching for reuse of demolition waste in construction projects; in German). *Grundwasser* 12 (2), 94–107.
- BGR (Bundesanstalt für Geowissenschaften und Rohstoffe), 2006. Nutzungsdifferenzierte Bodenübersichtskarte der Bundesrepublik Deutschland 1:1.000.000 (BÜK 1000 N2.3). Auszugskarten Acker, Grünland, Wald; (Land-use stratified soil map of Germany at a scale of 1:1.000.000 (BÜK 1000 N2.3). thematic maps cropland, pasture, forest; in German) Digit. Archiv FISBo BGR; Hannover and Berlin, Germany.
- Bigl, S.R., Berg, R.L., 1996. Testing of materials from the minnesota cold regions pavement research test facility. US Army Cold Regions Research and Engineering Laboratory (CRREL), Special Report 90-26. Hanover NH, USA. <http://www.crrel.usace.army.mil/techpub/CRREL_Reports/reports/SR96_20.pdf>.
- Bold, S., 2004. Processed-based prediction of long-term risk of groundwater pollution by organic non-volatile contaminants. PhD thesis, Tübinger Geowissenschaftliche Arbeiten (TGA), C72, University of Tübingen, Germany.
- Brakensiek, D.L., Rawls, W.J., 1994. Soil containing rock fragments: effects on infiltration. *Catena* 23 (1–2), 99–110.
- Carsell, R.F., Parish, R.S., 1988. Developing joint probability distributions of soil water retention characteristics. *Water Resources Research* 24 (5), 755–769.
- Delay, M., Lager, T., Schulz, H.D., Frimmel, F.H., 2007. Comparison of leaching tests to determine and quantify the release of inorganic contaminants in demolition waste. *Waste Management* 27 (2), 248–255.
- Du, Y., Wang, W., Kolditz, O., 2005. Richards flow modelling. 5. In: Workshop “Porous Media” Proceedings CD, second ed. Center for Applied Geosciences, University of Tübingen, Tübingen, Germany.
- FGSV, 1996. RAS-Q 96 Richtlinien für die Anlage von Straßen – Teil: Querschnitte. (Guidelines for the construction of roads – chapter: cross sections; in German). Köln, Germany.
- FGSV, 1997. ZTV E-StB 94, Zusätzliche Technische Vertragsbedingungen und Richtlinien für Erdarbeiten im Straßenbau. (Additional terms of contract and guidelines for ground works in road building; in German). Köln, Germany.
- FGSV, 1998. Merkblatt für wasserdurchlässige Befestigung von Verkehrsflächen. (Instructions for the stabilization of circulation areas permeable to water; in German). Köln, Germany.
- FGSV, 2004. ZTV SoB-StB 04 Zusätzliche Technische Vertragsbedingungen und Richtlinien für den Bau von Schichten ohne Bindemittel im Straßenbau. (Additional technical terms of contract and guidelines for the construction of unbound layers in road constructions; in German). Köln, Germany.
- FGSV, 2005. RAS-EW Richtlinien für die Anlage von Straßen – Teil: Entwässerung. (Guidelines for the construction roads – chapter: drainage; in German). Köln, Germany.
- Finkel, M., 1998. Quantitative Beschreibung des Transports von polyzyklischen aromatischen Kohlenwasserstoffen (PAK) und Tensiden in porösen Medien. (Quantitative description of the transport of polycyclic aromatic hydrocarbons (PAH) and surfactants in porous media; in German) PhD thesis, Tübinger Geowissenschaftliche Arbeiten (TGA), C47, University of Tübingen, Germany. http://w210.ub.uni-tuebingen.de/dbt/volltexte/2002/653/pdf/tgac47_diss_finkel.pdf.
- Finkel, M., Liedl, R., Teutsch, G., 1998. Modelling surfactant-enhanced remediation of polycyclic aromatic hydrocarbons. *Journal of Environmental Modelling and Software* 14, 203–211.
- Gluga, G., Jankiewicz, P., Rachimow, C., Lojek, K., Richter, K., Fürtig, G., Krahe, P., 2003. Wasserhaushaltsverfahren zur Berechnung vieljähriger Mittelwerte der tatsächlichen Verdunstung und des Gesamtabflusses. (Water balance method for the quantification of long-term averages of the actual evaporation and the total runoff; in German) Bundesanstalt für Gewässerkunde, BfG-Report 1342, Koblenz, Germany. <http://www.bafg.de/nn_163182/DE/02_Aufgabenfelder/01_Quantitative_Gewaesserkunde/01_Abteilung_Referate/M2_Ordnr/BAGLUVA_templateId=raw,property=publicationFile.pdf/BAGLUVA.pdf>.
- Grathwohl, P., 1992. Diffusion controlled desorption of organic contaminants in various soils and rocks. In: Kharaka, K.Y., Maest, A.S. (Eds.), *Water Rock Interaction – Proceedings of the Utah Conference*, pp. 283–286.
- Grathwohl, P., 1998. Diffusion in natural porous media: Contaminant transport, sorption/desorption and dissolution kinetics. Kluwer Academic Publishers, Boston, USA.
- Grathwohl, P., Susset, B., 2001. Sickerwasserprognose – Grundlagen, Möglichkeiten, Grenzen, Modelle. (Groundwater risk assessment – fundamentals, opportunities, limits, models; in German) In: *Belastung von Böden und Gewässern*, Gemeinschaftstagung ATV-DVWK, 28.-29.05.01, Hannover, Germany.
- Grathwohl, P., Liedl, R., Beyer, C., Konrad, W., 2006. Übertragung der Ergebnisse des BMBF – Förderschwerpunktes Sickerwasserprognose“ auf repräsentative Fallbeispiele (Förderkennzeichen 02WP0517). (Transfer of the results of the BMBF research priority “groundwater risk assessment” on representative case studies (Grant 02WP0517); in German) Final Report, University of Tübingen, Germany. <<http://edok01.tib.uni-hannover.de/edoks/e01fb07/527536415.pdf>>.
- Grathwohl, P., Halm, D., Bonilla, A., Broholm, M., Burganos, V., Christophersen, M., Comans, R., Gaganis, P., Gorostiza, I., Höhener, P., Kjeldsen, P., van der Sloot, H., 2003. Guideline for groundwater risk assessment at contaminated sites. Final Report EU-Project EVK1-CT-1999-00029. Campus Druck, Tübingen, Germany. <<http://www.uni-tuebingen.de/gracos/pdf/guideline.pdf>>.
- Hansson, K., 2005. Water and heat transport in road structures: development of mechanistic models. PhD thesis, Digital comprehensive summaries of Uppsala dissertations from the Faculty of Science and Technology, 23, Uppsala University, Sweden. <http://www.diva-portal.org/diva/getDocument?urn_nbn_se_uu_diva-4822-1_fulltext.pdf>.
- Hansson, K., Lundin, L.C., Simunek, J., 2006. Modeling water flow patterns in flexible pavements. *Transportation Research Record* 1936, 133–141.
- Hayduk, W., Laudie, H., 1974. Prediction of diffusion coefficients for nonelectrolytes in dilute aqueous solutions. *American Institute of Chemical Engineers Journal* 20 (3), 611–615.
- Hennings, V., 2000. Methodendokumentation Bodenkunde. Auswertungsmethoden zur Beurteilung der Empfindlichkeit und Belastbarkeit von Böden (Documentation of methods in soil science. Methods for evaluating the sensitivity and resilience of soils; in German). In: *Geologisches Jahrbuch/Sonderheft Reihe, G. (Ed.)*, second ed, vol. 1. Schweizerbart, Stuttgart, Germany.
- Henzler, R., 2004. Quantifizierung und Modellierung der PAK-Elution aus verfestigten und unverfestigten Abfallmaterialien (Quantification and modelling of the PAH-elution from solidified and unsolidified waste materials; in German) PhD thesis, Tübinger Geowissenschaftliche Arbeiten (TGA), C76, University of Tübingen, Germany. <http://w210.ub.uni-tuebingen.de/dbt/volltexte/2005/2028/pdf/Diss_Henzler_TGA76.pdf>.
- Henzler, R., Rügner, H., Grathwohl, P., 2006. Bewertung der Filter- und Pufferfunktion von Unterböden für organische Schadstoffe. (Filtering and buffering capacity of subsoils for organic contaminants; in German). *Bodenschutz* 1/2006, 8–14.
- Hjelmar, O., Holm, J., Crillessen, K., 2007. Utilisation of MSWI bottom ash as sub-base in road construction: First results from a large-scale test site. *Journal of Hazardous Materials* 139 (3), 471–480.

- Höhener, P., Dakhel, N., Christophersen, M., Broholm, M., Kjeldsen, P., 2006. Biodegradation of hydrocarbons vapors: Comparison of laboratory studies and field investigations in the vadose zone at the emplaced fuel source experiment, Airbase Værløse, Denmark. *Journal of Contaminant Hydrology* 88 (3–4), 337–358.
- Jaeger, R., Liedl, R., 2000. Prognose der Sorptionskinetik organischer Schadstoffe in heterogenem Aquifermaterial. (Prognosis of sorption kinetics of organic contaminants in heterogeneous aquifer materials; in German). *Grundwasser* 2, 57–66.
- Kellermann, C., 2003. Zur Bewertung des Infiltrationsverhaltens von Tragschichten ohne Bindemittel. (On the assessment of the infiltration behaviour of unbound base layers; in German) PhD thesis, Schriftenreihe des Lehrstuhls für Verkehrswegebau der Ruhr-Universität Bochum, Heft 19, University of Bochum, Germany.
- Kim, Y., Osako, M., 2003. Leaching characteristics of polycyclic aromatic hydrocarbons (PAHs) from spiked sandy soil. *Chemosphere* 51 (5), 387–395.
- Kleineidam, S., Rügner, H., Grathwohl, P., 1999a. Impact of grain scale heterogeneity on slow sorption kinetics. *Environmental Toxicology and Chemistry* 18 (8), 1673–1678.
- Kleineidam, S., Rügner, H., Ligouis, B., Grathwohl, P., 1999b. Organic matter facies and equilibrium sorption of phenanthrene. *Environmental Science and Technology* 33 (10), 1637–1644.
- Kolditz, O., Bauer, S., 2004. A process-oriented approach to computing multifield problems in porous media. *Journal of Hydroinformatics* 6 (3), 225–244.
- Kolditz, O., Beinhorn, M., Xie, M., Kalbacher, T., Bauer, S., Wang, W., McDermott, C., Chen, C., Beyer, C., Gronewold, J., Kemmler, D., Walsh, R., Du, Y., Park, C.H., Hess, M., Bürger, C., Delfs, J.-O., 2007. *GeoSys/Rockflow version 4.5.06 – Theory and users manual*, Center for Applied Geoscience, University of Tübingen, Germany.
- KrW-/AbfG, 1994. Gesetz zur Förderung der Kreislaufwirtschaft und Sicherung der umweltverträglichen Beseitigung von Abfällen (Kreislaufwirtschafts- und Abfallgesetz – KrW/AbfG). (Act for promoting closed substance cycle waste management and ensuring environmentally compatible waste disposal; in German) BGBl I 1994, 2705. <<http://bundesrecht.juris.de/bundesrecht/krw-abfg/gesamt.pdf>>.
- Lager, T., Delay, M., Karius, V., Hamer, K., Frimmel, F.H., Schulz, H.D., 2006. Determination and quantification of the release of inorganic contaminants from municipal waste incineration ash. *Acta hydrochimica et hydrobiologica* 34 (1–2), 73–85.
- Mesters, K., 1993. Abschätzung der Mobilisierbarkeit von leichtlöslichen Salzen aus Müllverbrennungsasche am Beispiel eines Lärmschutzwalles. (Estimation of the mobilizability of readily soluble salts from waste incineration ashes drawn on the example of a noise protection dam; in German) PhD thesis, Schriftenreihe des Lehrstuhls für Verkehrswegebau der Ruhr-Universität Bochum, Heft 5, University of Bochum, Germany.
- Mishra, S., Parker, J.C., Singhal, N., 1989. Estimation of soil hydraulic properties and their uncertainty from particle size distribution data. *Journal of Hydrology* 108, 1–18.
- Mualem, Y., 1976. A new model for predicting the hydraulic conductivity of unsaturated porous media. *Water Resources Research* 12, 513–522.
- Rügner, H., Henzler, R., Grathwohl, P., 2005. Beurteilung der Empfindlichkeit der Filter- und Pufferfunktion von Böden (i.B. Unterböden) nach Maßstäben des vorsorgenden Bodenschutzes für organische Schadstoffe. (Assessment of the sensitivity of the filtering and buffering capacity of soils (in particular subsoils) for organic contaminants according to the standards of preemptive soil protection; in German) Projekt: LABO 2003 B 2.03", Final Report, University of Tübingen, Germany. <http://www.laenderfinanzierungsprogramm.de/cms/WaBoAb_prod/WaBoAb/Vorhaben/LABO/B_2.03/lab-abschlussbericht-300305+final.pdf>.
- Rügner, H., Kleineidam, S., Grathwohl, P., 1997. Sorptions- und Transportverhalten organischer Schadstoffe in heterogenen Materialien am Beispiel des Phenanthrens. (Sorption and transport behaviour of organic contaminants in heterogeneous materials drawn on the example of phenanthrene; in German). *Grundwasser* 2 (3), 133–138.
- Rügner, H., Kleineidam, S., Grathwohl, P., 1999. Long-term sorption kinetics of phenanthrene in aquifer materials. *Environmental Science and Technology* 33 (10), 1645–1651.
- Schimmoller, V., Holtz, K., Eighmy, T., Wiles, C., Smith, M., Malasheskie, G., Rohrbach, G.J., Schaftlein, S., Campbell, R.D., Van Deusen, C.H., Ford, B., Almborg, J.A., 2000. *Recycled materials in European highway environments: uses, technologies, and policies*. Report No. FHWA-PL-00-025, Federal Highway Administration, US Department of Transportation, Washington DC, USA. <<http://international.fhwa.dot.gov/Pdfs/recycolor.pdf>>.
- Seth, R., Mackay, D., Muncke, J., 1999. Estimating of organic carbon partition coefficient and its variability for hydrophobic chemicals. *Environmental Science and Technology* 33 (14), 2390–2394.
- Stieber, M., Kraßnitzer, S., dos Santos Coutinho, C., Tiehm, A., 2006. Untersuchung der Bedeutung des mikrobiellen Abbaus für den Transport persistenter organischer Schadstoffe in der ungesättigten Zone (Förderkennzeichen O2WP0515). (Analysis of the relevance of microbial degradation for the transport of persistent organic contaminants in the unsaturated zone (Grant O2WP0515); in German) Final Report, DVGW Technologiezentrum Wasser (TZW), Karlsruhe, Germany. <<http://edok01.tib.uni-hannover.de/edoks/e01fb07/527534196.pdf>>.
- Stopпка, B., 2002. Prognose des Salzaustrags aus Straßenbaustoffen in der Sickerzone (Prognosis of the leaching of salts from road construction materials in the vadose zone; in German). PhD thesis, Schriftenreihe des Lehrstuhls für Verkehrswegebau der Ruhr-Universität Bochum, Heft 16, University of Bochum, Germany.
- Susset, B., 2007. *Materialien zur Sickerwasserprognose (Protocols for groundwater risk assessment; in German)*. In: Förstner, U., Grathwohl, P. (Eds.), *Ingenieurgeochemie Technische Geochemie - Konzepte und Praxis*, second ed. Springer, Berlin, Germany.
- Vanderborght, J., Vereecken, H., 2007. One-dimensional modeling of transport in soils with depth-dependent dispersion, sorption and decay. *Vadose Zone Journal* 6, 140–148.
- van Genuchten, M.T., 1980. A closed form equation for predicting the hydraulic conductivity of unsaturated soils. *Soil Science Society of America Journal* 44, 892–898.
- Wösten, J.H.M., Lilly, A., Nemes, A., Le Bas, C., 1998. Using existing soil data to derive hydraulic parameters for simulation models and in land use planning. SC-DLO, Agricultural Research Department, Winand Staring Centre for Integrated Land, Soil and Water Research, Report 156, Wageningen, The Netherlands.